

**INVESTIGATION OF THE STRUCTURE IN  
ELECTRODEPOSITED NANOSTRUCTURED Co/Cu  
ALLOYS, MULTILAYERS, AND CoFe/Cu  
MULTILAYERED NANOWIRES**

A Thesis

Submitted to the Graduate Faculty of the  
Louisiana State University and  
Agricultural and Mechanical College  
in partial fulfillment of the  
requirements for the degree of  
Master of Science

in

The Department of Chemistry

by  
Erick Jamal Lawson  
B.S. in Chemistry, Southern University and A & M College, May 2001  
May 2006

## ACKNOWLEDGMENTS

Over the past four years that I have been a graduate student at Louisiana State University, I would first like to thank God for giving me the opportunity to be here. Also, I would like to thank everyone who I was able to meet and intermingle with on a scientific and social level.

To begin with, I would like to thank my mom Pamela Wilkins as well as my grandmother Rosa Lee Wilkins. These two ladies, along with my son Brandon Jamal King, have been behind me 100% and have always been positive about me pursuing a higher education.

I am also thankful for Ms. Laurin Word. She has been there with me through good times and through bad. She has shown an insurmountable amount of patience while managing to remain very optimistic about having a future with me after the completion of my graduate studies.

My advisor, Dr. Julia Chan, has given me the necessary guidance to think critically and strive for the top as well as giving me the knowledge to know how the educational system works as a whole. Dr. Elizabeth Podlaha has been so patient in teaching me new things that was not initially part of her job and I thank her for that. I am also grateful for my collaborators Dr. David Young and his postdoc., Monica Moldovan, for helping my research along the way.

To finish, the rest of my fellow group members and departmental graduate students has made this experience that much better.

The work that is presented here was performed in part due to funding from LSU Capital and NSF-NIRT.

## TABLE OF CONTENTS

ACKNOWLEDGMENTS .....	ii
ABSTRACT.....	iv
CHAPTER	
1. INTRODUCTION .....	1
1.1 Magnetic Thin Films.....	1
1.1.1 Electrodeposition of Co/Cu Multilayered Thin Films .....	2
1.1.2 Electrodeposition of Co/Cu Alloy Thin Films.....	6
1.2 Magnetic Nanowires .....	8
1.2.1 Co Nanowires.....	10
1.2.2 Ni Nanowires .....	11
1.2.3 Fe Nanowires .....	11
1.2.4 Magnetic Multilayered Nanowires .....	13
2. ELECTRODEPOSITION OF Co/Cu MULTILAYERS .....	14
2.1 Experimental .....	15
2.2 X-Ray Diffraction.....	15
2.3 Results and Discussion .....	15
2.3.1 Structural Characterization of CoCu Alloys .....	15
2.3.2 Structural Characterization of Co/Cu Multilayers.....	18
3. ELECTRODEPOSITION OF CoFe/Cu MULTILAYERED NANOWIRES .....	20
3.1 Experimental.....	20
3.2 TEM Analysis .....	21
3.3 XRD Analysis .....	22
4. ATOMIC FORCE MICROSCOPY AND FUTURE OUTLOOK .....	24
REFERENCES .....	26
VITA.....	36

## ABSTRACT

Since the discovery of giant magnetoresistance (GMR) in electrodeposited nanostructured magnetic multilayers and multilayered nanowires, there has been interest throughout the scientific world in the fabrication and characterization of these materials. Magnetic multilayers in the form of thin films can be used as magnetoresistive sensors in the magnetic data storage industry. Arrays of nanowires have the potential for applications in perpendicular ultra-high density data storage and biosensors. Wire-shaped magnetic multilayered nanowires have been shown to exhibit GMR in the so called “current perpendicular-to plane” configuration (CPP-GMR). GMR of multilayers and multilayered nanowires have been investigated in several systems that include Co/Cu, Ni/Cu, NiFe/Cu, CoNi/Cu, and Fe/Cr.

In this work, the Co/Cu and CoFe/Cu systems were studied. These systems have produced nanometric multilayers that exhibit GMR, but it has yet to be reported that CoFe/Cu multilayered nanowires exhibit GMR. Our aim is to add Fe to the Co layer of Co/Cu multilayers and produce layers in the form of nanometric wires. The magnetic CoFe system has been chosen because of the combination of high magnetic moment (Co) and low magnetic anisotropy (Fe), two factors needed in order to optimize the GMR phenomenon. The wire-like shape of the nanowires will also serve as an easier way to measure CPP-GMR.

## CHAPTER 1. INTRODUCTION

### 1.1 Magnetic Thin Films

Nanostructured magnetic superlattices have been brought to the forefront of the information storage technology industry.[1] The term superlattice was coined originally to describe multilayers in which long range (longer than one bilayer thickness) structural coherence exists along the growth direction, but the two terms are frequently used interchangeably.[2] These materials are made of alternating layers of magnetic (i.e. Co, Fe, Ni, and their alloys) interleaved with nonmagnetic (i.e. Cu, Cr, Au, Ru) metals, and are often referred to as multilayers. Multilayers consist of two-dimensional (2D) entities of nanometer thicknesses. By varying the layer thickness, the properties of a superlattice can be significantly altered. For example, the electron spin arrangement of the magnetic layers is controlled by the precise thickness of the nonmagnetic layers. Furthermore, in multilayers where antiferromagnetic alignment of the magnetic layers is recognized, giant magnetoresistance (GMR) has been observed.[3] Nanostructured multilayers have been studied extensively due to their change in magnetoresistance comparing to their bulk constituents. GMR is defined as the “large” change in the resistance, of order 10-100%, of a material due to the application of a magnetic field. With the introduction of magnetoresistive (MR) data read heads, the read-back function of the head is now performed by a MR sensor.[4] As the performance parameters such as areal density increase, a demand has been created for materials with improved GMR and corrosive properties. Since the discovery of GMR in Fe/Cr multilayers [3] great strides have been made towards understanding process-structure-property relationships in materials to optimize this phenomenon. The fair control over the deposition parameters is needed,

since rough interfaces between subsequent layers may cause degradation of the GMR effect. There are multiple preparation techniques that have been used to fabricate magnetic multilayers. Sputtering [5], molecular beam epitaxy [6], evaporation in ultrahigh-vacuum [7], and electrodeposition [8-10] are the techniques that are most widely used. Each and every method has its own advantages and disadvantages when comparing the fabrication of the films that can be produced. In this manuscript, I will focus on the technique of electrodeposition.

### 1.1.1 **Electrodeposition of Co/Cu Multilayered Thin Films**

Electrodeposition (electroplating) refers to the deposition of a pure metal or alloy from an electrolyte solution by the passing of an electric current.[11] The morphological nature of the deposit is determined by several factors including the electrolyte composition, pH, temperature, agitation, and the current density. This process holds the advantages of being a continuous process with a high rate of deposition. It is also a room temperature process that is relatively inexpensive. With these advantages identified, electrodeposition has even been adopted by industry for preparation of magnetic materials and protective coatings.[4] Electrodeposition gives one control over the composition and structure by pulse plating. Pulse plating from a single electrolyte is done by using a periodically varying current or potential. Pulse plating can produce films with repeat lengths of the order of the nanometric scale, and with individual layers made of pure metals rather than alloys.[12] For example, cobalt and copper are interesting candidates for electrodeposited nanostructured superlattice studies because both elements are isostructural as bulk solids.

In 1987, Co/Cu multilayered structures were prepared from a single electrolyte bath.[8] X-ray diffraction (XRD) results indicated the presence of an FCC structure having a lattice constant intermediate to copper (3.615 Å) and cobalt (3.544 Å). No diffraction lines that could be attributed to HCP Co were found in the diffraction patterns. Co/Cu multilayered films were also obtained by the pulse electrodeposition method similar to that described by Dariel.[10] XRD patterns revealed two features: the absence of any reflections in a small-angle range and the presence of satellite reflections near the basic structure reflections of cobalt. XRD profiles have also been shown for [Co 2nm/Cu X nm]<sub>300</sub> multilayers fabricated by electrodeposition in the absence or presence of CrO<sub>3</sub>. [13] The XRD patterns show that for films grown in the absence of CrO<sub>3</sub>, the structure of Co is a mixture of FCC Co and HCP Co. For those in the presence of CrO<sub>3</sub>, with thicker Cu layer thickness of more than 0.5 nm, Co and Cu peaks are mainly FCC with a (111) texture. In 1989, antiferromagnetic coupling was found in Co/Cu superlattices, a common origin of GMR.[14] This sparked an immediate interest in the fabrication, structural, and physical property understanding of the Co/Cu multilayer regime. In 1995, the first evidence of GMR in pulse potentiostatic (potential control) electrodeposited multilayers was reported.[15] A GMR maximum of - 14% was measured in a field of 10 kOe. The highest room temperature GMR (- 55%) was found, in a field of <4.5 kOe, for a Co/Cu multilayer fabricated by electrodeposition.[16] The copper layers were varied in thickness from 0.5 to 8.0 nm, while the cobalt layers were maintained at a constant thickness of 3.2 nm. The relationship between the GMR and the copper layer thickness follows a sinusoidal function. The GMR value has a maximum when the copper layer thickness is ~0.8 nm. In 1996, the potentiostatic pulse method was

used to electrodeposit Co/Cu multilayers, and a small MR of - 0.9% was obtained in a small field of 1kOe.[17] Shortly thereafter, the pulse galvanostatic (current control) electrodeposition conditions required for the preparation of Co/Cu multilayers with compositional modulation, and the GMR of the films was investigated.[18] A maximum of GMR was found to be - 15%, at room temperature, in a field of 15 kOe. In 1997, a maximum GMR of - 18% was found, at room temperature, for a Co/Cu multilayer electrodeposited under potential control.[13] In 1998, a maximum of GMR was found to be - 4% at room temperature, in a field of 2 kOe, for a Co/Cu multilayer electrodeposited under potentiostatic control.[19] In the same year, a room temperature maximum of GMR (- 7.5%) was observed, in a field of 7 kOe, for a Co/Cu multilayer fabricated by potentiostatic electrodeposition.[20] In 1999, a maximum of GMR was found to be - 6% at room temperature, in a field of 7 kOe, for an electrodeposited multilayer of Co/Cu.[21] Shortly thereafter, a maximum GMR was found to be - 16%, at room temperature, for a Co/Cu multilayer that was electrodeposited by galvanostatic control.[22] In 2001, the GMR (- 15%) of a Co/Cu multilayer electrodeposited by potentiostatic control was maximized, at 77 K, in a field of 1.5 kOe.[23] That same year, a - 9% GMR maximum was observed for a Co/Cu multilayer produced by using electrodeposition with current control.[24] From these past results, it is known that the magnitude of GMR oscillates with the thickness of the individual layers. Hence, the better GMR values are obtained for a cobalt thickness that ranges from 1.5 – 3.5 nm and a copper thickness that ranges from 0.8 – 2.0 nm. The individual layer thickness for each sample reported above is in Table I.

Many studies have been reported on the preparation and characterization of electrodeposited Co/Cu multilayers in which the magnetic layer is, as a result of the nature of the electrodeposition method, not pure Co but rather a Co-rich Co-Cu alloy with magnetic properties very similar to those of pure Co.[8,9,15-18,25] In spite of these efforts, the observed room temperature GMR in electrodeposited Co/Cu multilayers has remained much smaller ( $< 20\%$ ) than values found in sputtered [26-28] Co/Cu multilayers. (The only exception is Ref. 16) So, the challenge remains to distinguish the parameters of electroplating that govern the GMR behavior of magnetic and nonmagnetic multilayers. It was found that the GMR of multilayer deposits decreased with increasing bilayer number, due to the deterioration of the microstructure as the deposit grew.[24] The bilayer number in the multilayers was varied between 700 and 1500. The general experience is that the multilayer interfaces are more pronounced at the beginning of the deposition than later, and after a few hundred of repeat periods, the original individual layer coherence is no longer as pronounced as in the initial phase. From the work discussed in this section, the corresponding bilayer number of each sample is listed in Table I. Hence, the GMR reaches its highest values in the bilayer number range of 300-800.

During the electrodeposition process, one drawback is the need to use a conductive substrate. A variety of substrates have been used for the electrodeposition of multilayers, and they include metal (i.e. Cu, Au) covered stainless steel disks [29], polycrystalline copper sheets [16], metal covered silicon wafers [15], metal covered glass plates [18], GaAs wafer [30], and titanium sheets.[24] As stated earlier, the highest room temperature GMR ( $\sim 55\%$ ) was found in an electrodeposited Co/Cu

multilayer deposited on a polycrystalline copper sheet.[16] Unfortunately, that work is widely criticized because it has not been able to be reproduced with comparable values. However, Cu proves to be the superior substrate for the fabrication of GMR multilayers that are reviewed in this section and listed in Table I.

The GMR values measured on the electrodeposited Co/Cu multilayered films have remained above - 20%, except for the work of Bird [16], regardless of the substrate used. To decrease cost of production, electrodeposition serves as a more economical route to produce these structures. Also, electrodeposition allows one to deposit into deep recesses [29], which is often needed for microdevice development. This research leaves an aim to systematically examine the electrochemical deposition parameters that will yield the most coherent multilayer structures accompanied with the largest GMR in the form of thin films.

Table I. Conditions for Multilayers Prepared by Electrodeposition

Author	Co Thickness (nm)	Cu Thickness (nm)	Bilayer #	Substrate	Magnetic Field, H (kOe)	GMR% at RT
Lenczowski	1.3	4	50	Cu covered Si	10	- 14
Bird	3.2	0.8	800-6000	Cu sheet	<4.5	- 55
Nallet	0.3	0.3	50	Au covered glass	1	- 0.9
Ueda 96'	1.5	1.4	50	Cu covered glass	15	- 15
Jyoko	2.0	3.2	300	Cu single crystal	10	- 18
Fannity	6.0	4.0	25	Cu covered glass	2	- 4
Shima	2.0	3.0	100	Cu covered Si	7	- 7.5
Nikitenko	1.6	4.0	200	Cu covered Si	7	- 6
Ueda 99'	0.9	1.4	50	Cu covered glass	21	- 16
Chassaing	0.8	4.5	20	ITO on glass	1.5	- 15 at 77 K
Péter	3.6	1.1	1325	Ti sheet	8	- 9

### 1.1.2 Electrodeposition of Co/Cu Alloy Thin Films

A brief synopsis of the CoCu alloy system is given here as a model system because of the inherently large GMR obtained with physical vapor deposition methods.

Thermodynamics show that cobalt and copper are immiscible [31], although in electrodeposited alloys metastable phases can exist, and examples are available for the CoCu system.[32-40] In Antón's study [33], it was shown that the lattice parameter followed Vegard's law when the composition of Co in the alloy increased from 2% to 25%, i.e. a linear relation of lattice parameter with composition. The presence of a solid solution was reported for granular alloys electrodeposited from citrate electrolytes, which also exhibited GMR.[38] The nature of CoCu electrodeposits is determined by many factors including the electrolyte composition, additive, pH, temperature and agitation, the potential or current density.[32-38,41] For example, it was reported that deposition current density has a significant control over the composition and microstructure, and that the pH of the electrolyte affects the morphology.[34] Auger Electron Spectroscopy (AES) depth profiling analysis showed that the CuCo film was not homogeneous; the bulk of the film was richer in Co while the surface and the bottom of the film was Co-poor.[32] The effects of additives sodium dodecylsulfate (SDS) and saccharin was during the pulsed deposition of CuCo alloys.[39] They found that SDS enhances Co displacement by Cu during open circuit conditions, while saccharin impedes this process. It was also reported that the addition of boric acid tends to increase the percentage of cobalt in the deposited alloys.[42] Others [36,37] have also investigated the GMR effect obtained when Co particles are embedded in the Cu matrix. It was reported that the GMR values depend sensitively on the Co particle size. A - 3 % maximum GMR value at 300 K, in a field of 17 kOe, was observed when the Co particle size is about 2.9 nm; the GMR was largely reduced when particle sizes are beyond 2.9 nm.

## 1.2 Magnetic Nanowires

The discovery of carbon nanotubes [43] started an enormous revolution in the interest of the synthesis and characterization of one-dimensional (1D) nanostructures. Nanometer-sized entities in the form of granular solids and superlattices are important materials because of their unusual properties compared to their bulk materials. Their interesting properties are directly related to the low dimensionality of the particles. On the other hand, a bulk solid is three-dimensional (3D). Since the discovery of GMR in electrodeposited nanostructured magnetic multilayered nanowires,[44,45] there has been interest throughout the scientific world in the fabrication and characterization of these materials. Many different techniques have been employed to produce nanowires. Among the various methods used for the fabrication of nanowires, template synthesis has proven to be the best approach and an alternative to other sophisticated nanophysics methods.[46] Template synthesis entails the filling of nanopores by electrochemical deposition of a material into the voids of some porous membrane. Electrodeposition is a versatile technique that provides a great advantage for industrial applications requiring high productivity and mass production at low processing cost with ambient conditions. Electrodeposition has proven to be the most suitable method for deposition into curved and recessed areas, which is needed for nanowire fabrication. Furthermore, the structural properties of electrodeposited nanowires are driven by a number of parameters which make possible their synthesis with a high reproducibility and different crystallographic structures of the same material in a controlled manner. Nanowire synthesis is usually performed through a nanoporous nonconductive template, usually made out of anodic aluminum oxide (AAO) or polycarbonate membranes, in order to form wires with high

aspect ratios. Sometimes these membranes are prepared by the user, and other times are commercially purchased. After deposition, the nanowires are set free from the template by dissolving the template in the correct solution. Nanowires represent an important class of 1D nanostructures that serve as models to study the structure-property relationship of materials that possess dimensionality and size constraints. Arrays of nanowires of ferromagnetic materials such as Co, Fe, and Ni have been studied intensely because of their potential applications in magnetic recording media, sensors, and other devices. Wire-shaped magnetic multilayered nanowires have been shown to exhibit GMR in the so called “current perpendicular-to plane” configuration (CPP-GMR). As the layers grow perpendicular to the axis of the substrate, CPP-GMR can easily be measured. Theory indicates that the physics of CPP-GMR is different from that of “current in the plane” (CIP-GMR).[47] In the CIP geometry, the GMR is significantly decreased when the layers thicknesses exceed the electron mean free path (a few nanometers). On the contrary, the layers do not need to be as thin in the CPP geometry, because the spin-diffusion lengths are the relevant scaling lengths (several tens of nanometers). These nanowires are usually a few tens of nanometers in diameter. Their properties are different than other artificially structured materials mentioned above because of their 1D nature. Applications require GMR effects at low field. In the upcoming sections of this report, I will review the previous work done on metallic nanowire systems and magnetic multilayered nanowire systems.

### 1.2.1 Co Nanowires

Co nanowires have been fabricated by electrodeposition into the pores of various membranes and formed vertical arrays of nanowires. Polyaniline nanotubes with the alumina membrane support as a “second-order-template”, has been used to prepare Co nanowires.[48] The array has uniaxial magnetic anisotropy with the easy axis parallel to the nanowires with the magnetization being perpendicular to the membrane. Polycarbonate membranes also serve as good host for Co nanowire arrays.[46,49-60] A magnetic field parallel or perpendicular to the membrane plane applied during deposition has been used to investigate how it controls the wire growth.[50] A magnetization reversal that depends on wire diameter has been found in Co nanowires that were deposited into polycarbonate membranes.[53] For small wire diameters, the easy axis is along the axis of the wires. As the wire diameter increases, the magnetization is reversed. Magnetotransport measurements on Co nanowires fabricated by electrodeposition into nanoporous polycarbonate membranes and contacted by electron beam lithography point out the inhomogeneous character of magnetic anisotropy and the reversal process in a single 60 nm Co nanowire.[60] The magnetic properties of an ordered array of concentric composite nanostructures of ZrO<sub>2</sub> nanotubules/Co nanowires containing a continuous and uniform Co nanowire in each ZrO<sub>2</sub> nanotubule have been reported.[61] FeCo [62], and CoNi [63] nanowires have been fabricated by electrodeposition in porous alumina films and magnetic studies performed on them. Ordered ferromagnetic-nonmagnetic alloys of (Co-Cu and Co-Ag),[64] and AgCuCo [65] nanowire arrays embedded in the channels of nanoporous anodic alumina membranes have also been fabricated by electrodeposition and their magnetic properties examined. The CoFe [66]

and CoNiFe [67] nanowire systems have been electrodeposited into polycarbonate membranes and their magnetic properties observed also.

### 1.2.2 Ni Nanowires

Electrodeposited Ni nanowires is another well-studied nanostructured system.[46,53,54,68-107] Carbon nanotubes that were initially deposited into porous alumina membranes served as a host for some ~4 nm diameter Ni nanowires, with an inner tubule diameter of 20 nm.[75] 100 nm periodic arrays of Ni nanowires showed that if one reduces the diameter of the nanowires from 55 to 30 nm, while keeping the interwire distance constant, coercive fields and remanence field is increased.[82] The magnetic alignment of electrodeposited Ni nanowires has been demonstrated and their response to the magnetic fields were quantified using video-microscopy.[84] Dynamic and static aspects of magnetization reversal in Ni nanowires have been examined along with their magnetic properties.[88] Ni nanowire arrays can also be electrodeposited into track-etched polymer membranes [46] and their magnetic properties studied.[53,54,71,73,77,105,108,109] Nanoporous single mica crystal membranes have also been used to produce Ni nanowire arrays with a diamond-shaped cross-section and ~120 nm diameter and 5 micron length, respectively.[85] The alloy systems of Ni-Cu [95] and NiFe [103,110] have been electrodeposited into anodic alumina membranes and their magnetic properties have been studied.

### 1.2.3 Fe Nanowires

Fe nanowires has been another widely studied system.[52,57,59,94,106,107,111-119] Fe nanowires that were electrodeposited into anodic aluminum oxide films had a coercivity that was found to be highly anisotropic and dependent upon the aspect ratio of

the particles.[111] Fe nanowires encapsulated within carbon nanotubes and their magnetic properties have also been investigated.[112] The protective carbon coating ensures that the metal is protected from oxidation. Magnetic moment orientations of  $\alpha$ -Fe nanowire arrays with two different diameters have been investigated.[114] Inside the  $\alpha$ -Fe nanowire array (60 nm in diameter) the magnetic moments are well parallel to the nanowires, but near the extremities of the nanowires the magnetic moment orientation deviates from parallelism to the long axis of the wire. When the diameter of the  $\alpha$ -Fe nanowires increases (300 nm in diameter), the angle of orientation between the moment direction and the long axis of the wire becomes larger near the extremities of the nanowire. Local spin-density-functional theory has been applied to describe the structural and magnetic properties of Fe nanowires consisting of chains of single atoms.[117] It is shown that an unsupported isolated wire is unstable with respect to both dimerization and bending. Magnetization reversal in arrays of parallel ferromagnetic Fe nanowires has also been examined.[119] The combination of magnetization measurements with field-dependent measurements showed that the macroscopic hysteresis loop was decomposed in terms of the irreversible magnetization response of individual nanowires. The magnetic hysteresis in arrays of Fe nanowires embedded in nanoporous alumina as a function of the template filling fraction has been investigated.[118] For partially filled membranes the shape anisotropy prevails and dipolar interactions between the nanowires are weak. Almost completely Fe-filled membranes show strong dipolar interactions that dominate the shape of the hysteresis loop.

#### 1.2.4 Magnetic Multilayered Nanowires

Electrodeposition of multilayered nanowires has been utilized to fabricate and study magnetic multilayered nanowires in several systems that include Co/Cu[44,45,120-132], Ni/Cu[133-135], NiFe/Cu[44,127,128,136], CoNi/Cu[137-139], and Fe/Cu[140] (for a review see reference [141]). The CPP-GMR of a [Co(7 nm)/Cu(3 nm)]<sub>500</sub> multilayered nanowire that was electrodeposited into the pores of a track-etched polycarbonate membrane was found to have a room temperature (RT) GMR of – 15%.[45] At 4.2 K, the GMR ratio was around – 19%, which is approximately 80% of the value at room temperature. These are closely related GMR ratios that have been observed by other authors too.[44,120] A RT CPP-GMR in the range of -15 to -20% was observed for a [CoNi(5 nm)/Cu(5 nm)]<sub>1500</sub> nanowire that was electrodeposited into the pores of a track-etched polycarbonate membrane.[137] A transmission electron microscopy (TEM) study has been done on Ni/Cu multilayers in the form of nanowires.[133] A [NiFe(12 nm)/Cu(4 nm)] nanowire that was electrodeposited into the pores of a track-etched polycarbonate membrane was observed to show a -20% GMR at RT and -80% at 4.2 K.[136] The CPP-GMR of a [Fe(8 nm)/Cu(10 nm)] multilayered nanowire that was electrodeposited into the pores of a track-etched polycarbonate membrane was found to have – 12% GMR at 5 K.[140] The first use of a nanoporous aluminum oxide membrane to electrodeposit multilayered nanowires proved to be extremely valuable.[139] A [CoNi(5.4 nm)/Cu(2.1 nm)] nanowire resulted in a – 55% CPP-GMR, compared to nothing more than – 20% for the same system electrodeposited in polycarbonate membranes.

## CHAPTER 2. ELECTRODEPOSITION OF Co/Cu MULTILAYERS

In the Co-Cu system, Cu is the more noble metal, meaning that it will reduce at a more positive reduction potential. Co is the less noble metal, that is, it has to be reduced with a more negative reduction potential. When a current is passed, an alloy rich copper layer will be produced if the molar concentrations and kinetic reaction rates of the metal ions in the solution are similar. Hence, the Cu concentration in solution has to be much lower than Co. At the onset of the applied current (low), a pure Cu layer will be produced, while at some more negative applied current, a Co-rich, Co-Cu alloy with pure Co properties will be deposited. A polarization curve is shown in Figure 2.1 as provided by Yutong Li (Graduate Student LSU Department of Chemical Engineering).

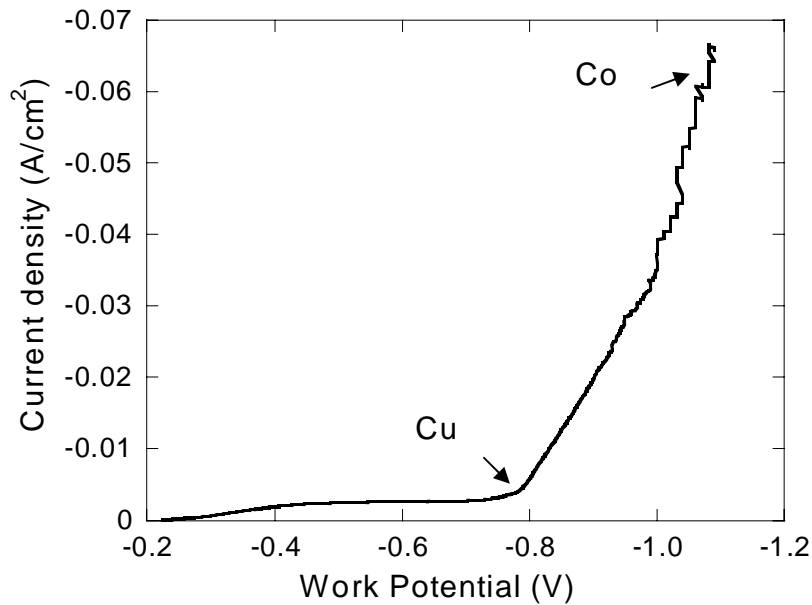


Figure 2.1 Polarization curve of the limiting current densities of cobalt and copper.

## 2.1 Experimental

In this work, CoCu alloys and multilayers were deposited on gold or stainless steel substrates and examined with X-ray diffraction (XRD). It has been shown that thick deposits of hundreds of bilayers result in a lowering of GMR.[24] However, thick films are of interest to MEMS-type devices where the GMR sensor material can also act as structural support. The growth of thick films, larger than one micron, become more sensitive to the electrolyte constituents and the plating parameters compared to the substrate surface. Therefore, the influence of Triton X-100 additive, and substrate is re-evaluated here for thick alloyed deposits.

## 2.2 X-Ray Diffraction

X-ray powder diffraction (XRD) data was obtained using a Bruker Advance D8 powder diffractometer equipped with a focusing Ge(*111*) incident beam monochromator (Cu  $K\alpha_1$  radiation) with a Bragg-Bretano geometry. The thin film-disk was placed on a glass-background quartz sample holder. X-ray diffraction data was obtained at ambient temperature in the range of  $2\theta = 35-55^\circ$  with a step range of  $0.02^\circ$  and a measuring time of 8 s per set. The full width at half maximum (fwhm) and d-spacings of the peaks was determined with DIFFRAC<sup>PLUS</sup> software by Bruker AXS.

## 2.3 Results and Discussion

### 2.3.1 Structural Characterization of CoCu Alloys

The XRD patterns of alloy samples, deposited at 400 rpm on Au covered stainless steel disks (SSD), at different current densities, show reflections of an FCC structure as shown in Figures 2.2(a) and 2.2(b), with the Triton X-100 additive. The Cu FCC peak shifts to higher  $2\theta$ , indicative of a decrease in lattice parameter as a consequence of Co

atoms substituted into the Cu matrix forming a solid solution. This agrees with results found in the literature.[33] No reflections of pure Co (neither HCP nor FCC) were observed. The lattice parameters calculated from the peak position are listed in the Table II. At low Co concentration, plated at lower current densities, the lattice parameter is close to that of pure Cu (3.615 Å) and decreases with increasing Co content plated at higher current densities. The average particle size was calculated using the classical Scherrer formulation.[142] The calculated results are also listed in Table II. The crystallite size of the deposit shows no correlation with Co content in the deposit as the current densities become larger. The calculated  $I_{(200)}/I_{(111)}$  ratio for elemental Cu is 0.46. The  $I_{(200)}/I_{(111)}$  ratio for  $\text{Cu}_{1-x}\text{Co}_x$  ( $x = 0.004$ ) is 0.59 and hence not significantly textured. However, the  $I_{(200)}/I_{(111)}$  ratio for  $\text{Cu}_{1-x}\text{Co}_x$  ( $x = 0.202$ ) is 0.79 which is significantly more textured than that of elemental Cu. For samples of  $\text{Cu}_{1-x}\text{Co}_x$  ( $x = 0.391 - 0.902$ ), the (200) reflection is not intense enough to obtain a calculated  $I_{(200)}/I_{(111)}$  ratio. Galvanostatic electrodeposition of Cu-Co alloys from a sulfate electrolyte has been examined over a broad range of compositions (0.39-94 wt. % Co) with a rotating disk electrode. XRD patterns showed a Co-Cu solid solution up to 90 wt. % Co.

Table II. Composition, Lattice Parameter, Ratio of  $I_{(200)}/I_{(111)}$ , Fwhm and Calculated Grain Size of Electrodeposited Alloys

Co %	Lattice Parameter (Å)	$I_{(200)}/I_{(111)}$	$2\theta/\text{fwhm}(\text{°})$	Grain Size (nm)
0.00	3.626(1)	0.29	43.174/ 0.161	53
0.40	3.615(1)	0.59	43.322/ 0.112	76
20.2	3.615(1)	0.79	43.315/ 0.102	116
39.1	3.613(1)	n/a	43.338/ 0.119	71
74.1	3.609(1)	n/a	43.391/ 0.177	48
79.9	3.610(1)	n/a	43.376/ 0.124	69
88.1	3.572(1)	n/a	43.863/ 0.087	98
90.2	3.549(1)	n/a	44.161/ 0.161	45

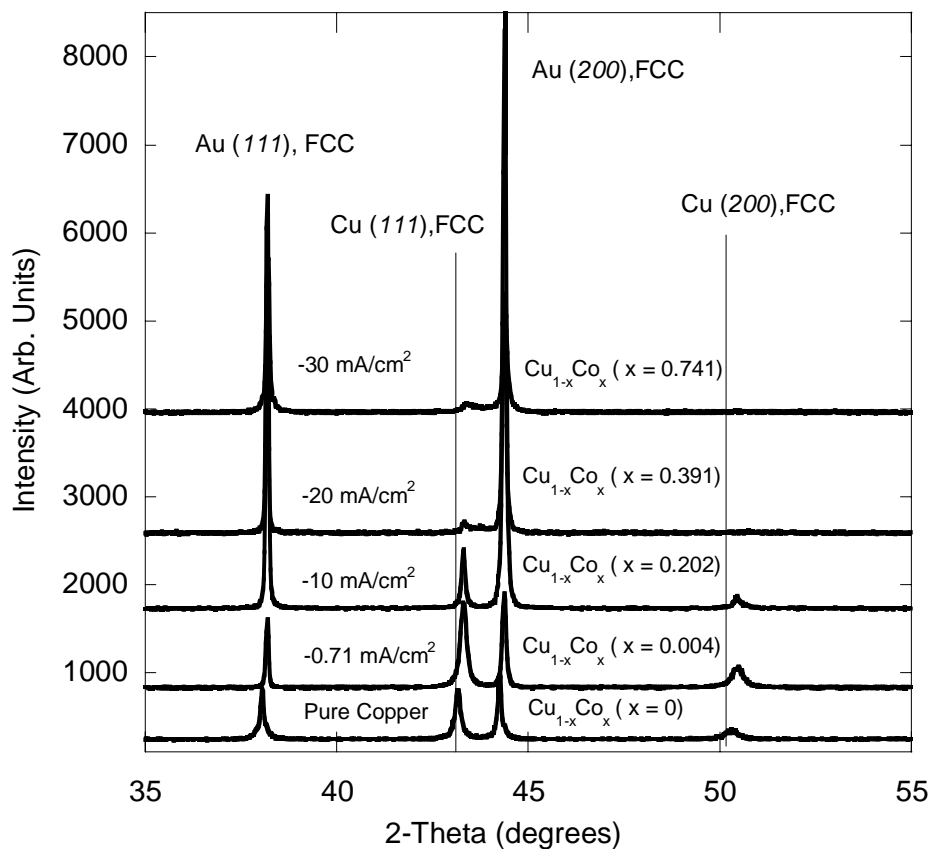


Figure 2.2(a) XRD of alloys deposited at low current densities.

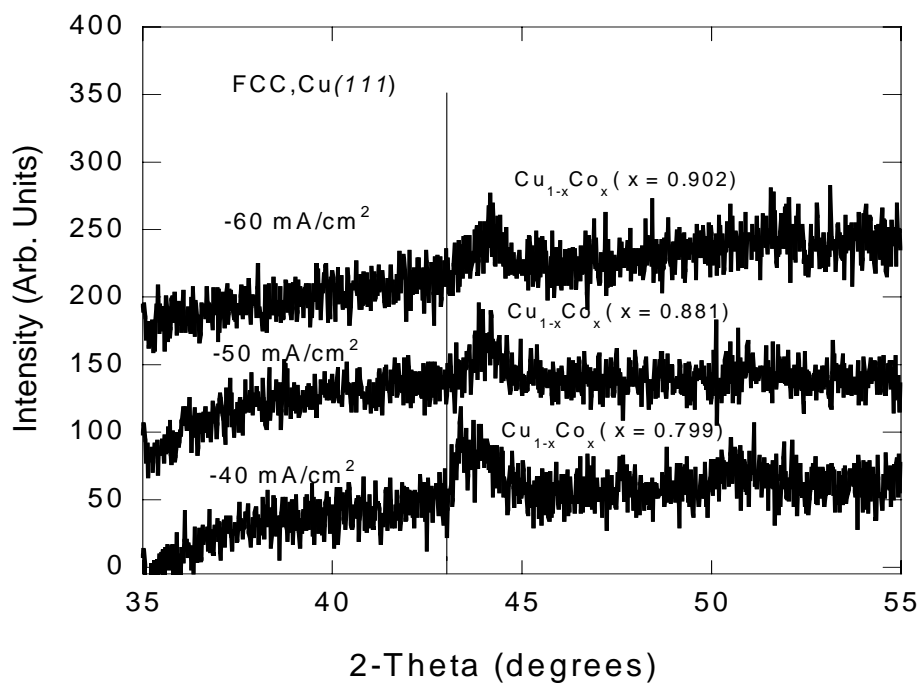


Figure 2.2(b) XRD of alloys deposited at high current densities.

### 2.3.2 Structural Characterization of Co/Cu Multilayers

The XRD analysis of the multilayers electrodeposited, on Au covered SSD, with different Cu-layer thickness is shown in Figure 2.3(a) and Figure 2.3(b). The lattice parameters and grain sizes are listed in Table III. In Figure 2.3(a) first order satellite peaks around the (111) main peak were observed for the 1.7 nm Cu thickness indicative of superlattice formation. When the Cu-rich layer is 0.7 nm there is a reduction of the intensity in the (111) peak, and no clear satellite peaks were observed, consistent with a loss of discrete layering. In Figure 2.3(b), when the copper layer thickness is 1.7 nm, no matter whether the Triton X-100 was used or not, on stainless steel, no satellite peak is observed for these two samples. The deviation of the FCC peak from the Cu FCC calculated value indicates significant alloying in the multilayer.

Table III. Composition, lattice parameter, ratio of  $I_{(200)}/I_{(111)}$ , fwhm and calculated grain size of electrodeposited multilayers

Composition	Lattice Parameter (Å)	$I_{(200)}/I_{(111)}$	2θ/fwhm(°)	Grain Size (nm)
[Cu 1.7 nm/Co 6 nm] <sub>500</sub> on Au SSD	3.591(1)	0.25	43.62/0.14	64
[Cu 0.7 nm/Co 6 nm] <sub>500</sub> on Au SSD	3.595(1)	n/a	43.53/0.22	94
[Cu 1.7 nm/Co 6 nm] <sub>500</sub> on SSD with Triton X- 100	3.591(1)	0.45	43.62/0.34	37
[Cu 1.7 nm/Co 6 nm] <sub>500</sub> on SSD without Triton X- 100	3.599(1)	0.29	43.57/0.09	41

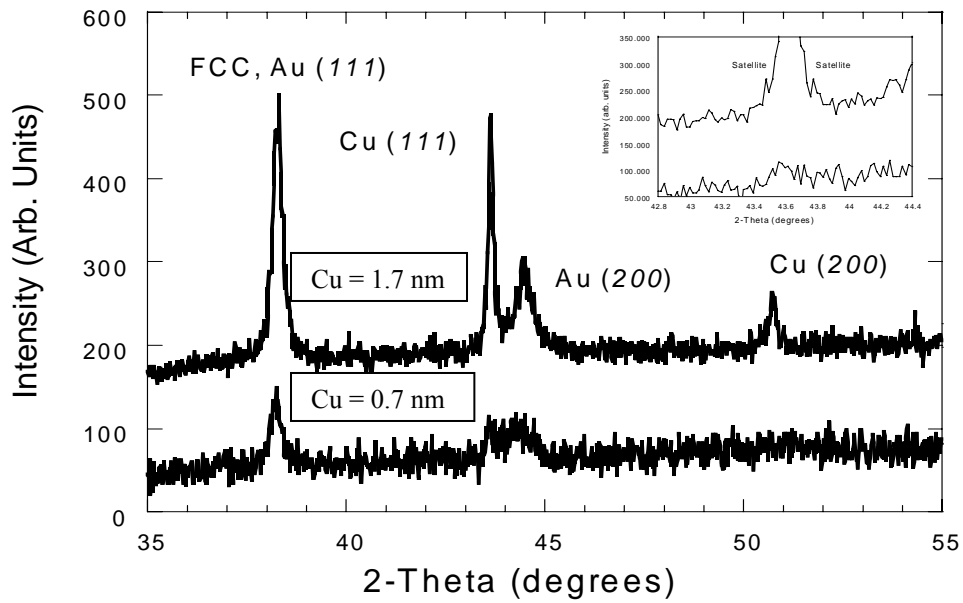


Figure 2.3(a) XRD of [Cu 1.7 nm/Co 6 nm]<sub>500</sub> (top) and [Cu 0.7 nm/Co 6 nm]<sub>500</sub> (bottom).

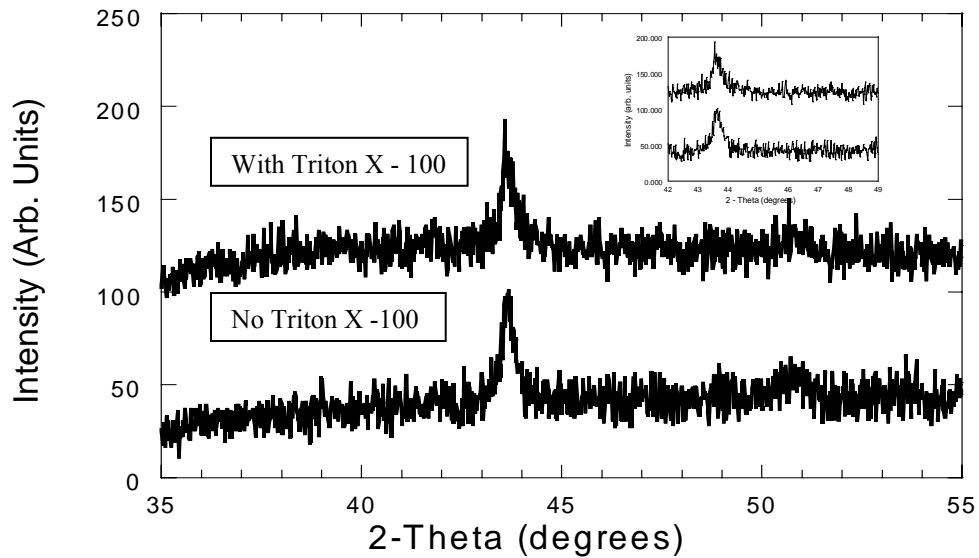


Figure 2.3(b) XRD of [Cu 1.7 nm/Co 6 nm]<sub>500</sub> film plated with Triton X -100 and without Triton X -100 on stainless steel disk.

## CHAPTER 3. ELECTRODEPOSITION OF CoFe/Cu MULTILAYERED NANOWIRES

In this particular work, the CoFe/Cu system will be of primary interest. This system has produced nanometric multilayers that exhibit GMR.[143-155] The magnetic CoFe layer has been chosen because of its high magnetic moment and low magnetic anisotropy in thin films.[156]

Even though there has been an extensive research effort on the electrodeposition of multilayered nanowires throughout different systems, no information has presently been disseminated for the electrodeposition of CoFe/Cu multilayered nanowires. In this work, I will explore the electrodeposition conditions that are required to fabricate CoFe/Cu multilayered nanowires.

### 3.1 Experimental

The electrolyte bath contains; 0.1 M  $\text{FeSO}_4 \cdot 7\text{H}_2\text{O}$ , 0.5 M  $\text{CoSO}_4 \cdot 7\text{H}_2\text{O}$ , 0.01 M  $\text{CuSO}_4 \cdot 5\text{H}_2\text{O}$ , 0.05 M  $\text{NaKC}_4\text{H}_4\text{O}_6 \cdot 4\text{H}_2\text{O}$ , and 0.6 g/L of Triton X – 100. The pH was kept at (~3.0). Commercially available AAO membranes were used for nanowire deposition. A layer of  $\text{Au}_{60}\text{Pd}_{40}$  alloy was sputtered by an Edwards S150 sputter coater on one side of the membrane to seal the pores and serve as the counter electrode for the electrolyte solution. A stationary holder was used to hold the membrane in place, with no agitation, for the plating process. Following deposition, a 1 M NaOH solution was used to dissolve the membrane, in order to set the wires free from the membrane. The liquid was then put in the centrifuge, and NaOH was taken out of the sample by pipet. Distilled water was then added to the sample and put in the centrifuge again to spin off any excess NaOH. Two microliters was then put on a copper/carbon grid specially designed for transmission electron microscopy (TEM) and allowed to dry. The grid was then put in

the JEOL 100 CX TEM for morphology analysis. XRD was used to determine the crystallographic structure of the nanodeposits.

### 3.2 TEM Analysis

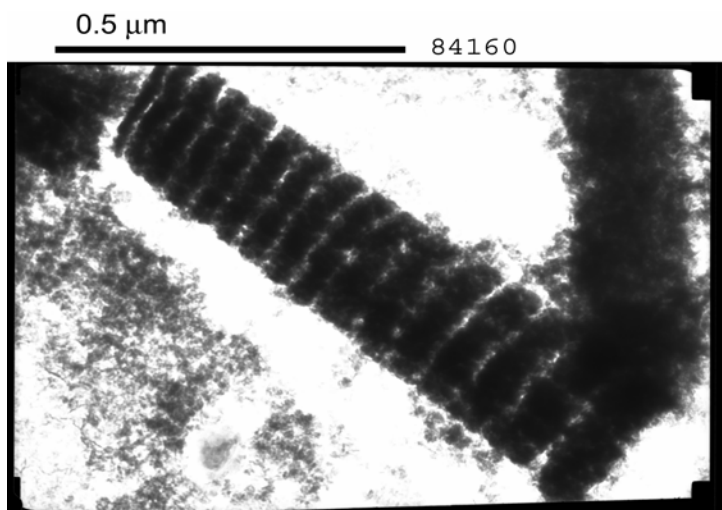


Figure 3.1 A TEM picture of a multilayered nanowire of CoFe/Cu showing distinct CoFe-rich (light bands) and Cu-rich (dark bands) layers

The TEM figure above clearly shows a layered structure was fabricated. The magnification bar is on a scale of 500 nm. The light layers (~15 nm) are represented by CoFe which was plated at a deposition potential of -1.9 V for 4 seconds. The dark layers (~50 nm) are represented by the Cu layer which was plated at a deposition potential of -0.5 V for 100 seconds. This particular wire diameter is ~220 nm. The wire diameter (measured from TEM) is greater than the nominal pore diameter. Others have revealed such a discrepancy between the nominal pore size and the measured pore size diameters and considered the manufacturers as the reason for indefiniteness of the nanopore size determination.[69] The electrodeposition of a CoFe/Cu multilayer has been clearly observed within the nanopores of alumina membranes.

### 3.3 XRD Analysis

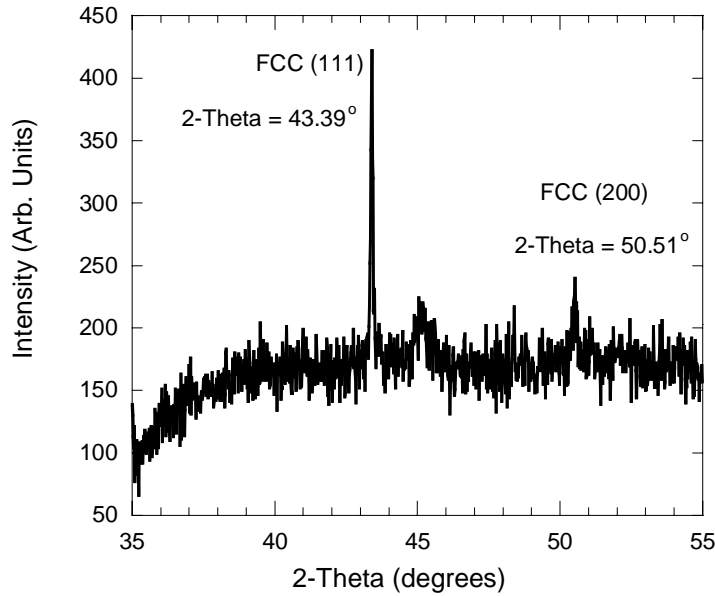


Figure 3.2 A XRD pattern of a CoFe/Cu multilayered nanowire embedded in anodic aluminum oxide (AAO)

The XRD pattern of a CoFe/Cu multilayered nanowire (pictured in figure 5) deposited into AAO is shown in Figure 6. The relative intensity  $I_{(200)}/I_{(111)}$  is experimentally calculated to be 0.57, versus a 0.46 theoretical intensity. The calculated lattice parameter is 3.608(1) Å for  $2\theta = 43.39^\circ$ , which is slightly smaller than the lattice of pure Cu (3.615 Å), is expected because of the addition of the smaller lattice Co and Fe into the deposit. The FCC (200) reflection is shown at  $2\theta = 50.51^\circ$ . The reflection at  $2\theta = 45.05^\circ$  is indicative of FCC (111) Co. The deviation of the FCC (111) Co peak from the Co FCC (111) calculated value indicates that there is some alloying going on within the multilayered structure. The calculated lattice parameter of 3.608(1) Å for the FCC (111) Cu reflection is close to the lattice parameter of 3.609(1) Å which is recognized in the Co solid solution experiment that was done back in chapter two. The 3.609(1) Å

lattice corresponds to 74.1% Co in the Co-Cu alloys. This indicates that this sample has ~74.1 wt. % Co-Cu alloy at the interface in its deposit.

## CHAPTER 4. ATOMIC FORCE MICROSCOPY AND FUTURE OUTLOOK

The atomic force microscope (AFM) is a combination of the principles of the scanning tunneling microscope and the stylus profilometer.[157] It incorporates a probe that does not damage the surface. AFM has become a prevalent tool for observing surfaces, molecules, biological cells and nanometer size particles at the atomic level.[158-160] For example, AFM images using AC tapping mode are shown below in Figure 7. The sample is an unfilled porous anodic aluminum oxide (AAO) membrane commercially available at Whatman Company, Inc. (Cat. No. 6809-6002) The membranes are 25 mm in diameter with each pore size ( $\sim 0.02 \mu\text{m}$ ), respectively.

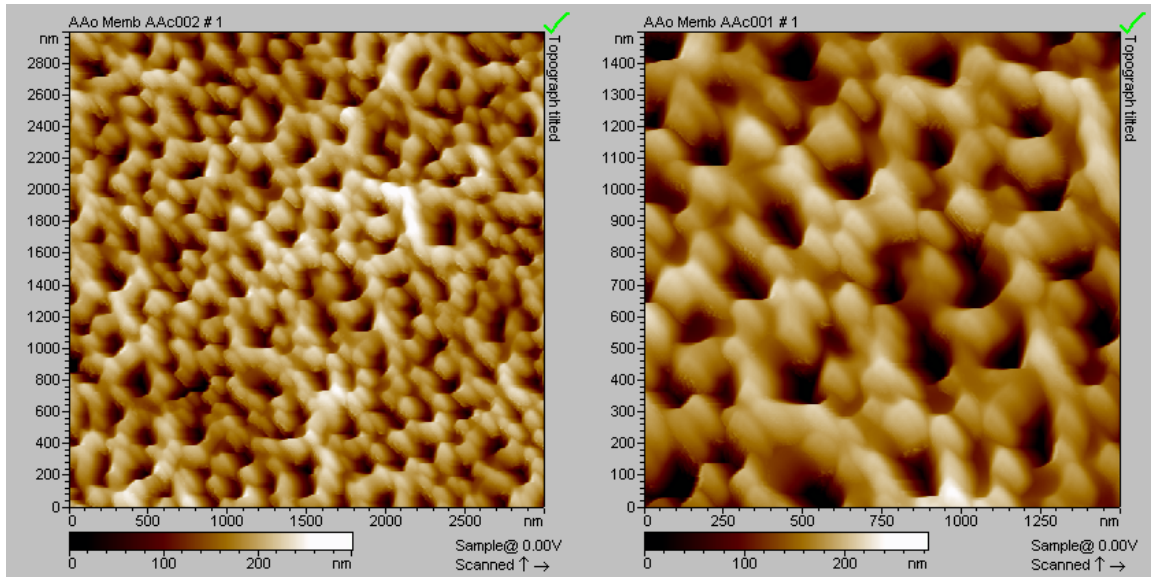


Figure 4.1 AC tapping mode image of the surface of an AAO membrane acquired in air. (left) Wide area view ( $3 \times 3 \text{ mm}^2$ ) displays the arrangement and variations of pore sizes; (right) Zoom-in view ( $1.5 \times 1.5 \text{ mm}^2$ ).

Various imaging modes have given AFM the ability to measure vertical and lateral deflections with striking resolution and extremely small force sensitivity. These attributes make AFM powerful in investigating properties of surfaces and of different complex systems on surfaces. In this chapter, I will discuss a new technique (which has

not yet been published) that will allow one to detect ultra small magnetic forces induced by magnetic vibration of magnetic or ferromagnetic nanoparticles, and use AFM to map out such nanoparticles on or near the surface. This imaging mode can be termed Magnetic Acoustic Probe (MAP Mode) Microscopy.

MAP Mode-AFM uses a modulated magnetic field to cause magnetic nanoparticles to vibrate. A magnetic field is applied to the samples which are placed on a special MAP Mode sample plate. An AC current is applied to a coil of wire, which induces a magnetic field. This field will shake materials that are magnetic. A standard silicon nitride AFM tip which does not have any magnetic coating is used for standard contact mode imaging. The instrument feedback adjusts the tip-sample distance for a constant applied force. The mechanical vibration of the magnetic nanoparticles drives the AFM tip to vibrate at the same frequency when it is in direct contact or in close vicinity. Topographic images are obtained using a constant force mode imaging technique. A lock-in amplifier is used to selectively acquire the amplitude and phase of the AC component consistent with the driving frequency, in order to eliminate the topographic factor. By reconstruction of both the amplitude and phase signal simultaneously with the topographic image, images of the surface magnetic acoustic response can be mapped with high resolution. Nanometric magnetic particles located on or near the sample surface can be mapped using MAP Mode. The MAP Mode-AFM to map the location of the magnetic nanoparticles, their size, their mass, linking to the environment and their interaction between each other in Co, Ni, and CoNi nanostructured magnetic nanowires fabricated into commercial AAO templates.

## REFERENCES

- [1] C. H. Tsang, R. E. Fontana Jr., T. Lin, D. E. Heim, B. A. Gurney, M. L. Williams, *IBM J. Res. Develop.* 42 (1998) 103.
- [2] I. K. Schuller, *Solid State Commun.* 92 (1994) 141.
- [3] M. N. Baibich, J. M. Broto, A. Fert, F. Nguyen Van Dau, F. Petroff, P. Eiteene, G. Creuzet, A. Friederich, J. Chazelas, *Phys. Rev. Lett.* 61 (1988) 2472.
- [4] P. C. Andricacos, N. Robertson, *IBM J. Res. Develop.* 42 (1998) 671.
- [5] A. R. Modak, S. S. P. Parkin, D. J. Smith, *J. Magn. Magn. Mater.* 129 (1994) 415.
- [6] F. J. Lamelas, C. H. Lee, H. He, W. Vavra, R. Clarke, *Phys. Rev. B* 40 (1989) 5837.
- [7] J. P. Renard, P. Beauvillain, C. Dupas, K. Le Dang, P. Veillet, E. Vélú, C. Marlière, D. Renard, *J. Magn. Magn. Mater.* 115 (1992) L147.
- [8] M. Dariel, L. H. Bennett, D. S. Lashmore, P. Lubitz, M. Rubinstein, W. L. Lechter, M. Z. Harford, *J. Appl. Phys.* 61 (1987) 4067.
- [9] R. D. McMicheal, U. Atzmony, C. Beauchamp, L. H. Bennett, L. J. Swartzendruber, D. S. Lashmore, Romanikiw, *J. Magn. Magn. Mater.* 113 (1992) 149.
- [10] V. M. Fedosyuk, O. I. Kasyutich, *J. Magn. Magn. Mater.* 125 (1993) 330.
- [11] C. A. Ross, *Annu. Rev. Mater. Sci.* 24 (1994) 159.
- [12] D. M. Tench, J. T. White, *J. Electrochem. Soc.* 137 (1990) 3061.
- [13] Y. Jyoko, S. Kashiwabara, Y. Hayashi, *J. Electrochem. Soc.* 144 (1997) L5.
- [14] A. Cebollada, J. L. Martínez, J. M. Gallego, J. J. de Miguel, R. Miranda, S. Ferrer, F. Batallán, G. Fillion, J. P. Rebouillat, *Phys. Rev. B* 39 (1989) 9726.
- [15] S. K. J. Lenczowski, C. Schönenberger, M. A. M. Gijs, W. J. M. de Jonge, *J. Magn. Magn. Mater.* 148 (1995) 455.
- [16] K. D. Bird, M. Schlesinger, *J. Electrochem. Soc.* 142 (1995) L65.
- [17] P. Nallet, E. Chassaing, M. G. Walls, M. J. Hÿtch, *J. Appl. Phys.* 79 (1996) 6884.
- [18] Y. Ueda, N. Hataya, H. Zaman, *J. Magn. Magn. Mater.* 156 (1996) 350.

- [19] H. El Fanity, K. Rahmouni, M. Bouanani, A. Dinia, G. Shmerber, C. Mény, P. Panissod, Á. Cziráki, F. Cherkaoui, A. Berrada, *Thin Solid Films* 318 (1998) 227.
- [20] M. Shima, L. Salamanca - Riba, T. P. Moffat, R. D. McMichael, L. J. Swartzendruber, *J. Appl. Phys.* 84 (1998) 1504.
- [21] V. I. Nikitenko, V. S. Gornakov, L. M. Dedukh, A. F. Khapikov, T. P. Moffat, A. J. Shapiro, R. D. Shull, M. Shima, L. Salamanca - Riba, *J. Magn. Magn. Mater.* 198-199 (1999) 477.
- [22] Y. Ueda, N. Kikuchi, S. Ikeda, T. Houga, *J. Magn. Magn. Mater.* 198-199 (1999) 740.
- [23] E. Chassaing, *J. Electrochem. Soc.* 148 (2001) C690.
- [24] L. Péter, Á. Cziráki, L. Pogány, Z. Kupay, I. Bakonyi, M. Uhlemann, M. Herrich, B. Arnold, T. Bauer, K. Wetzig, *J. Electrochem. Soc.* 148 (2001) C168.
- [25] E. A. M. Van Alphen, A. H. J. Colaris, S. K. J. Lenczowski, C. Schönenberger, W. J. M. de Jonge, *J. Magn. Magn. Mater.* 156 (1996) 29.
- [26] S. S. P. Parkin, R. Bhadra, K. P. Roche, *Phys. Rev. Lett.* 66 (1991) 2152.
- [27] S. S. P. Parkin, Z. G. Li, D. J. Smith, *Appl. Phys. Lett.* 58 (1991) 2710.
- [28] D. H. Mosca, F. Petroff, A. Fert, P. A. Schroeder, W. P. Pratt Jr., R. Laloe, *J. Magn. Magn. Mater.* 94 (1991) L1.
- [29] Q. Huang, D. P. Young, J. Y. Chan, J. Jiang, E. J. Podlaha, *J. Electrochem. Soc.* 149 (2002) C349.
- [30] K. Attenborough, H. Boeve, J. De Boeck, G. Borghs, J.-P. Celis, *Appl. Phys. Lett.* 74 (1999) 2206.
- [31] *Alloy Phase Diagrams*. ASM International, Ohio (1992).
- [32] T. Cohen-Hyams, W. D. Kaplan, D. Aurbach, Y. S. Cohen, J. Yahalom, *J. Electrochem. Soc.* 150 (2003) C28.
- [33] R. L. Antón, M. L. Fdez-Gubieda, A. García-Arribas, J. Herreros, M. Insausti, *Mater. Sci. Eng. A* 335 (2002) 94.
- [34] G. R. Pattanaik, D. K. Pandya, S. C. Kashyap, *J. Electrochem. Soc.* 149 (2002) C363.

- [35] K. Miyazaki, S. Kainuma, K. Hisatake, T. Watanabe, N. Fukumuro, *Electrochim. Acta* 44 (1999) 3713.
- [36] H. Errahmani, A. Berrada, G. Schemerber, A. Dinia, *J. Magn. Magn. Mater.* 238 (2002) 147.
- [37] W. Wang, F. Zhu, W. Lai, J.-q. Wang, G. Yang, J. Zhu, Z. Zhang, *J. Phys. D: Appl. Phys.* 32 (1999) 1990.
- [38] E. Gómez, A. Labarta, A. Llorente, E. Vallés, *J. Electroanal. Chem.* 517 (2001) 63.
- [39] J. J. Kelly, P. Kern, D. Landolt, *J. Electrochem. Soc.* 147 (2002) 3725.
- [40] P. E. Bradley, D. Landolt, *Electrochim. Acta* 45 (1999) 1077.
- [41] R. López, J. Herreros, A. García-Arribas, J. M. Barandiarán, M. L. Fdez-Gubieda, *J. Magn. Magn. Mater.* 196-197 (1999) 53.
- [42] S. S. Abd EI-Rehim, S. M. Abd EI-Wahab, S. M. Rashwan, Z. M. Anwar, *J. Chem. Technol. Biot.* 75 (2000) 237.
- [43] S. Iijima, *Nature* 354 (1991) 56.
- [44] A. Blondel, J. P. Meier, B. Doudin, J.-P. Ansermet, *Appl. Phys. Lett.* 65 (1994) 3019.
- [45] L. Piraux, J. M. George, J. F. Despres, C. Leroy, E. Ferain, R. Legras, K. Ounadjela, A. Fert, *Appl. Phys. Lett.* 65 (1994) 2484.
- [46] T. M. Whitney, J. S. Jiang, P. C. Searson, C. L. Chien, *Science* 261 (1993) 1316.
- [47] T. Valet, A. Fert, *Phys. Rev. B* 48 (1993) 7099.
- [48] H. Cao, Z. Xu, H. Sang, D. Sheng, C. Tie, *Adv. Mater.* 13 (2001) 121.
- [49] A. Encinas, M. Demand, J. M. George, L. Piraux, *IEEE Trans. Magn.* 38 (2002) 2574.
- [50] S. Ge, C. Li, X. Ma, W. Li, L. Xi, C. X. Li, *J. Appl. Phys.* 90 (2001) 509.
- [51] S. Kumar, R. Kumar, S. K. Chakarvarti, *J. Mater. Sci.* 39 (2004) 2951.
- [52] V. Langlais, S. Arrii, L. Pontonnier, G. Tourillon, *Scripta Mater.* 44 (2001) 1315.

- [53] K. Ounadjela, R. Ferré, L. Louail, J. M. George, J. L. Maurice, L. Piraux, S. Dubois, *J. Appl. Phys.* 81 (1997) 5455.
- [54] L. Piraux, S. Dubois, E. Ferain, R. Legras, K. Ounadjela, J. M. George, J. L. Maurice, A. Fert, *J. Magn. Magn. Mater.* 165 (1997) 352.
- [55] J. Rivas, A. Kadazi Mukenga Bantu, G. Zaragoza, M. C. Blanco, M. A. López-Quintela, *J. Magn. Magn. Mater.* 249 (2002) 220.
- [56] V. Scarani, B. Doudin, J.-P. Ansermet, *J. Magn. Magn. Mater.* 205 (1999) 241.
- [57] G. Tourillon, L. Pontonnier, J. P. Levy, V. Langlais, *Electrochem. Solid State Lett.* 3 (2000) 20.
- [58] L. Vila, J. M. George, G. Faini, A. Popa, U. Ebels, K. Ounadjela, L. Piraux, *IEEE Trans. Magn.* 38 (2002) 2577.
- [59] J. Verbeeck, O. I. Lebedev, G. Van Tendeloo, L. Cagnon, C. Bougerol, G. Tourillon, *J. Electrochem. Soc.* 150 (2003) E468.
- [60] L. Vila, L. Piraux, J. M. George, G. Faini, *Appl. Phys. Lett.* 80 (2002) 3805.
- [61] J. Bao, C. Tie, Z. Xu, Q. Ma, J. Hong, H. Sang, D. Sheng, *Adv. Mater.* 14 (2002) 44.
- [62] L. Menon, S. Bandyopadhyay, Y. Liu, H. Zeng, D. J. Sellmyer, *J. Nanosci. Nanotech.* 1 (2001) 149.
- [63] H. Zhu, S. Yang, G. Ni, D. Yu, Y. Du, *Scripta Mater.* 44 (2001) 2291.
- [64] Y. W. Wang, L. D. Zhang, G. W. Meng, X. S. Peng, Y. X. Jin, J. Zhang, *J. Phys. Chem. B* 106 (2002) 2502.
- [65] V. M. Fedosyuk, O. I. Kasyutich, W. Schwarzacher, *J. Magn. Magn. Mater.* 198-199 (1999) 246.
- [66] I. Shao, C. Cammarata, and P. C. Searson, *Proceedings of the 7<sup>th</sup> Symposium of Magnetic Materials Processes and Devices*, (2003) 461.
- [67] G. C. Han, B. Y. Zong, Y. H. Wu, *IEEE Trans. Magn.* 38 (2002) 2562.
- [68] M. Vázquez, K. Pirola, M. Hernández-Vélez, V. M. Prida, D. Navas, R. Sanz, F. Batallán, J. Velázquez, *J. Appl. Phys.* 95 (2004) 6642.
- [69] I. Chlebny, B. Doudin, J.-P. Ansermet, *Nanostruct. Mater.* 2 (1993) 637.

- [70] M. Lederman, R. O'Barr, S. Schultz, IEEE Trans. Magn. 31 (1995) 3793.
- [71] J. P. Meier, B. Doudin, J.-P. Ansermet, J. Appl. Phys. 79 (1996) 6010.
- [72] R. O'Barr, M. Lederman, S. Schultz, W. Xu, A. Scherer, R. J. Tonucci, J. Appl. Phys. 79 (1996) 5303.
- [73] W. Wernsdorfer, K. Hasselbach, A. Benoit, B. Barbara, B. Doudin, J. P. Meier, J.-P. Ansermet, D. Mailly, Phys. Rev. B 55 (1997) 11552.
- [74] R. O'Barr, S. Schultz, J. Appl. Phys. 81 (1997) 5458.
- [75] B. K. Pradhan, T. Kyotani, A. Tomita, Chem. Commun. 14 (1999) 1317.
- [76] M. Zheng, L. Menon, H. Zeng, Y. Liu, S. Bandyopadhyay, R. D. Kirby, D. J. Sellymer, Phys. Rev. B 62 (2000) 12282.
- [77] S. Pignard, G. Goglio, A. Radulescu, L. Piraux, S. Dubois, A. Declémy, J. L. Duvail, J. Appl. Phys. 87 (2000) 824.
- [78] K. Nielsch, F. Müller, A.-P. Li, Gösele, Adv. Mater. 12 (2000) 582.
- [79] M. Zheng, R. Skomski, Y. Liu, D. J. Sellymer, J. Phys.: Condens. Matter 12 (2000) L497.
- [80] A. J. Yin, J. Li, W. Jian, A. J. Bennett, J. M. Xu, Appl. Phys. Lett. 79 (2001) 1039.
- [81] H. Cao, C. Tie, Z. Xu, J. Hong, H. Sang, Appl. Phys. Lett. 78 (2001) 1592.
- [82] K. Nielsch, R. B. Wehrspohn, J. Barthel, J. Kirschner, U. Gösele, S. F. Fischer, H. Kronmüller, Appl. Phys. Lett. 79 (2001) 1360.
- [83] A. Encinas-Oropesa, M. Demand, L. Piraux, I. Huynen, U. Ebels, Phys. Rev. B 63 (2001) 104415.
- [84] M. Tanase, L. A. Bauer, A. Hultgren, D. M. Silevitch, L. Sun, D. H. Reich, P. C. Searson, G. J. Meyer, Nano Lett. 1 (2001) 155.
- [85] L. Sun, P. C. Searson, C. L. Chien, Appl. Phys. Lett. 79 (2001) 4429.
- [86] H. Zeng, S. Michalski, R. D. Kirby, D. J. Sellymer, L. Menon, S. Bandyopadhyay, J. Phys.: Condens. Matter 14 (2002) 715.

- [87] K. Nielsch, R. B. Wehrspohn, J. Barthel, J. Kirschner, S. F. Fischer, H. Kronmüller, T. Schweinböck, D. Weiss, U. Gösele, *J. Magn. Mater.* 249 (2002) 234.
- [88] H. Zeng, R. Skomski, L. Menon, Y. Liu, S. Bandyopadhyay, D. J. Sellymer, *Phys. Rev. B* 65 (2002) 134426.
- [89] F. Elhoussine, S. Mátéfi-Tempfli, A. Encinas, L. Piraux, *Appl. Phys. Lett.* 81 (2002) 1681.
- [90] Z. K. Wang, M. H. Kuok, S. C. Ng, D. J. Lockwood, M. G. Cottam, K. Neilsch, R. B. Wehrspohn, U. Gösele, *Phys. Rev. Lett.* 89 (2002) 027201.
- [91] S. Melle, J. L. Menéndez, G. Armelles, D. Navas, M. Vázquez, K. Nielsch, R. B. Wehrspohn, U. Gösele, *Appl. Phys. Lett.* 83 (2003) 4547.
- [92] Y.-T. Pang, G.-W. Meng, W.-J. Shan, Q. Fang, L.-D. Zhang, *Chin. Phys. Lett.* 20 (2003) 144.
- [93] K.-H. Xue, G.-P. Pan, M.-H. Pan, M. Lu, G.-H. Wang, *Supperlattices and Microstructures* 33 (2003) 119.
- [94] C. G. Jin, W. F. Liu, C. Jia, X. Q. Xiang, W. L. Cai, L. Z. Yao, X. G. Li, *J. Crystal Growth* 258 (2003) 337.
- [95] Y. G. Guo, L. J. Wan, C. F. Zhu, D. L. Yang, D. M. Chen, C. L. Bai, *Chem. Mater.* 15 (2003) 664.
- [96] S. W. Lin, S. C. Chang, R. S. Liu, S. F. Hu, N. T. Jan, *J. Magn. Mater.* 282 (2004) 28.
- [97] H. Y. Zhang, X. Gu, X. H. Zhang, X. Ye, X. G. Gong, *Phys. Lett. A* 331 (2004) 332.
- [98] S. Kato, H. Kitazawa, G. Kido, *J. Magn. Mater.* 272-276 (2004) 1666.
- [99] M. Vázquez, M. Hernández-Vélez, K. Pirola, A. Asenjo, D. Navas, J. Velázquez, P. Vargas, C. A. Ramos, *Eur. Phys. J. B* 40 (2004) 489.
- [100] S.-K. Hwang, S.-H. Jeong, O.-J. Lee, K.-H. Lee, *Microelectron Eng.* 77 (2005) 2.
- [101] H. Pan, B. Liu, J. Yi, C. Poh, S. Lim, J. Ding, Y. Feng, C. H. A. Huan, J. Lin, *J. Phys. Chem. B* 109 (2005) 3094.

- [102] C. A. Ross, M. Hwang, M. Shima, H. I. Smith, M. Farhoud, T. A. Savas, W. Schwarzacher, J. Parrochon, W. Escoffier, H. N. Bertram, F. B. Humphrey, M. Redjdal, *J. Magn. Magn. Mater.* 249 (2002) 200.
- [103] H. Chiriac, A. E. Moga, M. Urse, T.-A. Óvári, *Sensors and Actuators A* 106 (2003) 348.
- [104] J. Xu, X. Huang, G. Xie, Y. Fang, D. Liu, *Materials Research Bulletin* 39 (2004) 811.
- [105] R. Ferré, K. Ounadjela, J. M. George, L. Piraux, S. Dubois, *Phys. Rev. B* 56 (1997) 14066.
- [106] P. M. Paulus, F. Luis, M. Kröll, G. Schmid, L. J. de Jongh, *J. Magn. Magn. Mater.* 224 (2001) 180.
- [107] M. Kröll, W. J. Blau, D. Grandjean, R. E. Benfield, F. Luis, P. M. Paulus, L. J. de Jongh, *J. Magn. Magn. Mater.* 249 (2002) 241.
- [108] J. P. Meier, A. Blondel, B. Doudin, J.-P. Ansermet, *Helvetica Phys. Acta* 67 (1994) 761.
- [109] W. Wernsdorfer, B. Doudin, D. Mailly, K. Hasselbach, A. Benoit, J. P. Meier, J.-P. Ansermet, B. Barbara, *Phys. Rev. Lett.* 77 (1996) 1873.
- [110] Z. Hao, Y. Shaoguang, N. Gang, Y. Dongliang, D. Youwei, *J. Magn. Magn. Mater.* 234 (2001) 454.
- [111] D. AlMawlawi, N. Coombs, M. Moskovits, *J. Appl. Phys.* 70 (1991) 4421.
- [112] N. Grobert, W. K. Hsu, Y. Q. Zhu, J. P. Hare, H. W. Kroto, D. R. M. Walton, M. Terrones, H. Terrones, P. Redlich, M. Rühle, R. Escudero, F. Morales, *Appl. Phys. Lett.* 75 (1999) 3363.
- [113] T. Kishi, H. Nakanishi, H. Kasai, W. A. Diño, F. Komori, *Jpn. J. Appl. Phys.* 42 (2003) 4633.
- [114] F. Li, L. Ren, Z. Niu, H. Wang, T. Wang, *J. Phys.: Condens. Matter* 14 (2002) 6875.
- [115] R. M. Metzger, V. V. Konovalov, M. Sun, T. Xu, G. Zangari, B. Xu, M. Benakli, W. D. Doyle, *IEEE Trans. Magn.* 36 (2000) 30.
- [116] Y. Peng, H.-L. Zhang, S.-L. Pan, H.-L. Li, *J. Appl. Phys.* 87 (2000) 7405.
- [117] D. Spišák, J. Hafner, *Phys. Rev. B* 65 (2002) 235405.

- [118] T. G. Sorop, K. Nielsch, P. Göring, M. Kröll, W. J. Blau, R. B. Wehrspohn, U. Gösele, L. J. de Jongh, *J. Magn. Magn. Mater.* 272-276 (2004) 1656.
- [119] T. G. Sorop, C. Untiedt, F. Luis, M. Kröll, M. Rasa, L. J. de Jongh, *Phys. Rev. B* 67 (2003) 014402.
- [120] B. Voegeli, A. Blondel, B. Doudin, J.-P. Ansermet, *J. Magn. Magn. Mater.* 151 (1995) 388.
- [121] K. Liu, K. Nagodawithana, P. C. Searson, C. L. Chien, *Phys. Rev. B* 51 (1995) 7381.
- [122] L. Piraux, S. Dubois, A. Fert, *J. Magn. Magn. Mater.* 159 (1996) L287.
- [123] L. Piraux, S. Dubois, C. Marchal, J. M. Beuken, L. Filipozzi, J. F. Despres, K. Ounadjela, A. Fert, *J. Magn. Magn. Mater.* 156 (1996) 317.
- [124] C. Beeli, B. Doudin, J.-P. Ansermet, P. Stadelmann, *J. Magn. Magn. Mater.* 164 (1996) 77.
- [125] B. Doudin, A. Blondel, J.-P. Ansermet, *J. Appl. Phys.* 79 (1996) 6090.
- [126] A. Blondel, B. Doudin, J.-P. Ansermet, *J. Magn. Magn. Mater.* 165 (1997) 34.
- [127] L. Piraux, S. Dubois, J. L. Duvail, K. Ounadjela, A. Fert, *J. Magn. Magn. Mater.* 175 (1997) 127.
- [128] S. Dubois, J. M. Beuken, L. Piraux, J. L. Duvail, A. Fert, J. M. George, J. L. Maurice, *J. Magn. Magn. Mater.* 165 (1997) 30.
- [129] B. Doudin, J. E. Wegrowe, S. E. Gilbert, V. Scarani, D. Kelly, J. P. Meier, J.-P. Ansermet, *IEEE Trans. Magn.* 34 (1998) 968.
- [130] L. Piraux, S. Dubois, A. Fert, L. Belliard, *Eur. Phys. J. B* 4 (1998) 413.
- [131] T. Ohgai, X. Hoffer, A. Fábíán, L. Gravier, J.-P. Ansermet, *J. Mater. Chem.* 13 (2003) 2530.
- [132] T. Ohgai, X. Hoffer, L. Gravier, J. E. Wegrowe, J.-P. Ansermet, *Nanotechnology* 14 (2003) 978.
- [133] L. Wang, K. Yu-Zhang, A. Metrot, P. Bonhomme, M. Troyon, *Thin Solid Films* 288 (1996) 86.
- [134] A. Robinson, W. Schwarzacher, *J. Appl. Phys.* 93 (2003) 7250.

- [135] M. Chen, P. C. Searson, C. L. Chien, *J. Appl. Phys.* 93 (2003) 8253.
- [136] S. Dubois, C. Marchal, J. M. Beuken, L. Piraux, J. L. Duvail, A. Fert, J. M. George, J. L. Maurice, *Appl. Phys. Lett.* 70 (1997) 396.
- [137] A. Blondel, J. P. Meier, B. Doudin, J.-P. Ansermet, K. Attenborough, P. Evans, R. Hart, G. Nabiyouni, W. Schwarzacher, *J. Magn. Magn. Mater.* 148 (1995) 317.
- [138] G. P. Heydon, S. R. Hoon, A. N. Farley, S. L. Tomlinson, M. S. Valera, K. Attenborough, W. Schwarzacher, *J. Phys. D: Appl. Phys.* 30 (1997) 1083.
- [139] P. R. Evans, G. Yi, W. Schwarzacher, *Appl. Phys. Lett.* 76 (2000) 481.
- [140] S. Dubois, E. Chassaing, J. L. Duvail, L. Piraux, M. G. Waals, *J. Chim. Phys.* 96 (1999) 1316.
- [141] A. Fert, L. Piraux, *J. Magn. Magn. Mater.* 200 (1999) 338.
- [142] B. D. Cullity, *Elements of X-ray Diffraction*. Addison-Wesley, (1978) 555.
- [143] Y. Saito, K. Inomata, *Jpn. J. Appl. Phys.* 30 (1991) L1733.
- [144] Y. Saito, S. Hashimoto, K. Inomata, *IEEE Trans. Magn.* 28 (1992) 2751.
- [145] Y. Saito, S. Hashimoto, K. Inomata, *Appl. Phys. Lett.* 60 (1992) 2436.
- [146] K. Inomata, Y. Saito, *Appl. Phys. Lett.* 61 (1992) 726.
- [147] K. Inomata, Y. Saito, *J. Magn. Magn. Mater.* 126 (1993) 425.
- [148] N. Kataoka, K. Saito, H. Fujimori, *J. Magn. Magn. Mater.* 121 (1993) 383.
- [149] H. Kanai, R. L. White, *IEEE Trans. Magn.* 29 (1993) 2729.
- [150] K. Inomata, Y. Saito, S. Hashimoto, *J. Magn. Magn. Mater.* 121 (1993) 350.
- [151] M. R. Parker, S. Hossain, D. Seale, J. A. Barnard, M. Tan, H. Fujiwara, *IEEE Trans. Magn.* 30 (1994) 358.
- [152] Y. Seyama, A. Tanaka, M. Oshiki, *IEEE Trans. Magn.* 35 (1999) 2838.
- [153] Y. Chen, S. Wang, L. Mei, K. Rhie, S. Byeun, *J. Mater. Sci. Technol.* 18 (2002) 436.

- [154] E. B. Svedberg, K. J. Howard, M. C. Bønsanger, B. B. Pant, A. G. Roy, D. E. Laughlin, *J. Appl. Phys.* 94 (2003) 1001.
- [155] S. H. Florez, R. D. Gomez, *IEEE Trans. Magn.* 39 (2003) 34113413.
- [156] D. Wang, J. Anderson, J. M. Daughton, *IEEE Trans. Magn.* 33 (1997) 3520.
- [157] G. Binnig, C. F. Quate, C. H. Gerber, *Phys. Rev. Lett.* 56 (1986) 930.
- [158] A. Paul, T. Damm, D. E. Bürgler, S. Stein, H. Kohlstedt, P. Grünberg, *Appl. Phys. Lett.* 82 (2003) 1905.
- [159] Y. Zhang, M. Floyd, K. P. Driver, J. Drucker, P. A. Crozier, D. J. Smith, *Appl. Phys. Lett.* 80 (2002) 3623.
- [160] I. J. Lee, J. W. Kim, T. B. Hur, Y. H. Hwang, H. K. Kim, *Appl. Phys. Lett.* 81 (2002) 475.

## VITA

Erick Lawson was born in Lake Charles, Louisiana on September 13, 1979. He graduated from Lake Charles Boston High School, in 1997, in the top five percentile of his class. He went on to attend Southern University Agricultural and Mechanical College and majored in chemistry. He earned a Bachelor of Science degree in chemistry, with honors, by the spring of 2001. After that, he enrolled at Louisiana State University to pursue an advanced degree. Erick will be graduating with a Master of Science in chemistry from Louisiana State University in the spring of 2006.